MICROMACHINED STIMULATING ELECTRODES

Quarterly Report #1

(Contract NIH-NINDS-N01-NS-5-2335)

October 1995 --- December 1995

Submitted to the

Neural Prosthesis Program
National Institute of Neurological Disorders and Stroke
National Institutes of Health

by the

Center for Integrated Sensors and Circuits
Department of Electrical Engineering and Computer Science
University of Michigan
Ann Arbor, Michigan
48109-2122

February 1996

MICROMACHINED STIMULATING ELECTRODES

Summary

During the past quarter, work on the development of thin-film micromachined stimulating electrode arrays has gone forward in a number of areas. Three additional process runs of active and passive probes have been fabricated for internal and external users. Histological studies of an 8-site passive probe implanted for approximately six weeks showed biological material adhering selectively to each of the exposed sites, all of which passed some current during the implant period. Another electrode, recovered from a similar test, was not used for stimulation for at least four weeks prior to sacrifice and did not show tissue accumulation on any of its sites. For another chronically-implanted multisite probe, the in-vivo cyclic voltammetry curves, the in-vivo impedances, and the in-vivo access resistances remained relatively stable and viable after 18 weeks of implantation. The instrumentation for making many of these measurements is being upgraded to allow impedance spectroscopy on the electrodes along with improved data collection capabilities. Work has also begun to improve the contact and interconnect structures used on the probes. This includes the use of TiN and Ti:W contact plugs and refractory metal/silicide low-resistance interconnects. Sputtering targets for the selected materials have been ordered, and a test mask set to allow technology development is in design.

The current-generation circuitry used on STIM-2 is being redesigned to allow more reliable current sinking capabilities and to ensure more accurate matching between the source and sink currents. A number of different circuit designs are being simulated, and a final design should be completed during the coming term. Yield problems associated with an aluminum hillocking problem on some of the bonding pads in STIM-2 are also being corrected.

The design of a new 64-site 4-channel active stimulating probe (STIM-2b) is nearing completion. This device uses a 20b serial input word to control four 16:1 site selectors, resulting in a 64:4 site multiplexer. The selected site from each of the four groups can be either passed directly to an output pad for connection to an external current generator or can be passed to the pad through an on-chip preamplifier, allowing neural activity in the vicinity of the site to be monitored externally. A new fabrication run of the previous STIM-1a and STIM-1b probes has begun, and a run of the revised STIM-2 probe and the new STIM-2b probe will begin during the coming quarter.

MICROMACHINED STIMULATING ELECTRODES

1. Introduction

The goal of this research is the development of active multichannel arrays of stimulating electrodes suitable for studies of neural information processing at the cellular level and for a variety of closed-loop neural prostheses. The probes should be able to enter neural tissue with minimal disturbance to the neural networks there and deliver highly-controlled (spatially and temporally) charge waveforms to the tissue on a chronic basis. The probes consist of several thin-film conductors supported on a micromachined silicon substrate and insulated from it and from the surrounding electrolyte by silicon dioxide and silicon nitride dielectric films. The stimulating sites are activated iridium, defined photolithographically using a lift-off process. Passive probes having a variety of site sizes and shank configurations have been fabricated successfully and distributed to a number of research organizations nationally for evaluation in many different research preparations. For chronic use, the biggest problem associated with these passive probes concerns their leads, which must interface the probe to the outside world. Even using silicon-substrate ribbon cables, the number of allowable interconnects is necessarily limited, and yet a great many stimulating sites are ultimately desirable in order to achieve high spatial localization of the stimulus currents.

The integration of signal processing electronics on the rear of the probe substrate (creating an "active" probe) allows the use of serial digital input data which can be demultiplexed on the probe to provide access to a large number of stimulating sites. Our goal in this area has been to develop a family of active probes capable of chronic implantation in tissue. For such probes, the digital input data must be translated on the probe into per-channel current amplitudes which are then applied to the tissue through the sites. Such probes require five external leads, virtually independent of the number of sites used. As discussed in our previous reports, we are now developing a series of active probes containing CMOS signal processing electronics. Two of these probes are slightly redesigned versions of an earlier first-generation set of designs and are designated as STIM-1a and STIM-1b. The third probe, STIM-2, is a second-generation version of our high-end first-generation design, STIM-1. All three probes provide 8-bit resolution in setting the per-channel current amplitudes. STIM-1A and -1B offer a biphasic range using ±5V supplies from 0μA to ±254μA with a resolution of 2μA, while STIM-2 has a range from 0 to ±127μA with a resolution of 1μA. STIM-2 offers the ability to select 8 of 64 electrode sites and to drive these sites independently and in parallel, while -1a allows only 2 of 16 sites to be active at a time (bipolar operation). STIM-1b is a monopolar probe, which allows the user to guide an externally-provided current to any one of 16 sites as selected by the digital input address. The high-end STIM-2 contains provisions for numerous safety checks and for features such as remote impedance testing in addition to its normal operating modes. It also offers the option of being able to record from any one of the selected sites in addition to stimulation.

During the past quarter, we have continued to fabricate passive probe structures for internal and external users. No further problems with iridium adhesion have been experienced. Electrical and histological studies have been performed on short- and long-term in-vivo implants of passive stimulating probes, and the development of improved contract and interconnect structures has also been initiated. The redesign of the current generation circuitry on STIM-2 is proceeding, and improvements in the external interface

circuitry have been made. A new stimulating probe, STIM-2b, is also being designed. The results in each of these areas are described below.

2. *In-Vivo Stimulation with Passive Probes*

Several areas were worked on during this past quarter. Two electrodes were retrieved from implants and examined using a scanning electron microscope. A chronically implanted electrode was tested periodically and is currently operational in its fourth month. New hardware and software was developed to improve and expand data collection.

The goal of the chronic stimulation experiments is to measure the electrical parameters of the electrode-tissue system under conditions of bipolar and monopolar stimulation using a multisite stimulating electrode. It is theorized that site size, the presence or absence of a probe shank between the sites, and the encapsulating tissue may affect the current path between the sites and that changes in this path can be detected by measuring electrical characteristics. Several electrical parameters are monitored. These include bipolar and monopolar impedance, bipolar and monopolar access resistance, anodic voltage, cathodic voltage, and charge storage. These measurements provide information about the condition of both the tissue and the electrode sites.

Short-Term In-Vivo Studies

The experimental protocol will first be reviewed briefly. A chronic stimulating electrode is implanted in the occipital lobe of an adult guinea pig. Two different probe designs were used in the experiments. One was an eight-site four-shank device with site sizes of 400, 800, 1200, and 1600μm^2. Site pairs of the same size were grouped on a shank. The other probe had three shanks and six 1000μm^2 sites. After a 10 day rest period, the stimulation protocol began. Each bipolar pair was stimulated for 4 hours a day for five days. The stimulus waveform was a biphasic pulse of 50μA magnitude, 0.1 msec/phase duration, and 250Hz rate. Impedance was taken at 1kHz, using a 5μA sine wave. A 0.6V bias was placed on the sites inbetween pulses to place the electrode in the most favorable charge transfer state. Four weeks after the last day of stimulation the animal is sacrificed for tissue histology and electrode evaluation.

The electrical data from these experiments was presented in previous reports. This report contains histological data from a retrieved electrode. Figure 1 shows all eight sites of an electrode. Figure 2 shows a close up of a single site. Clearly, a substance specific to the electrode site has accumulated on every site. Elemental analysis using the SEM in the Microbeam Analysis Laboratory showed that the material on the site had higher than nominal levels of carbon and oxygen, which suggests that the material is biological in nature. This phenomenon was noted in earlier reports. In those reports, it was suggested that only sites that were used to pass current were covered with tissue. Not all the eight sites in Fig. 1 were stimulated chronically, yet all did pass current at some point. Impedances were checked and cyclic voltammetry was performed on all sites. The accumulation of tissue on the sites does not appear to be specific to sites used for chronic stimulation. Another electrode was recovered from a similar test, but did not show tissue accumulation on any sites. However, this electrode was not functional at the time of sacrifice, and, therefore, the sites were not active for four weeks before sacrifice. This suggests that the tissue accumulation may be a transient phenomenon. One variable that could be tested is the time interval between use of the site and sacrifice of the animal.

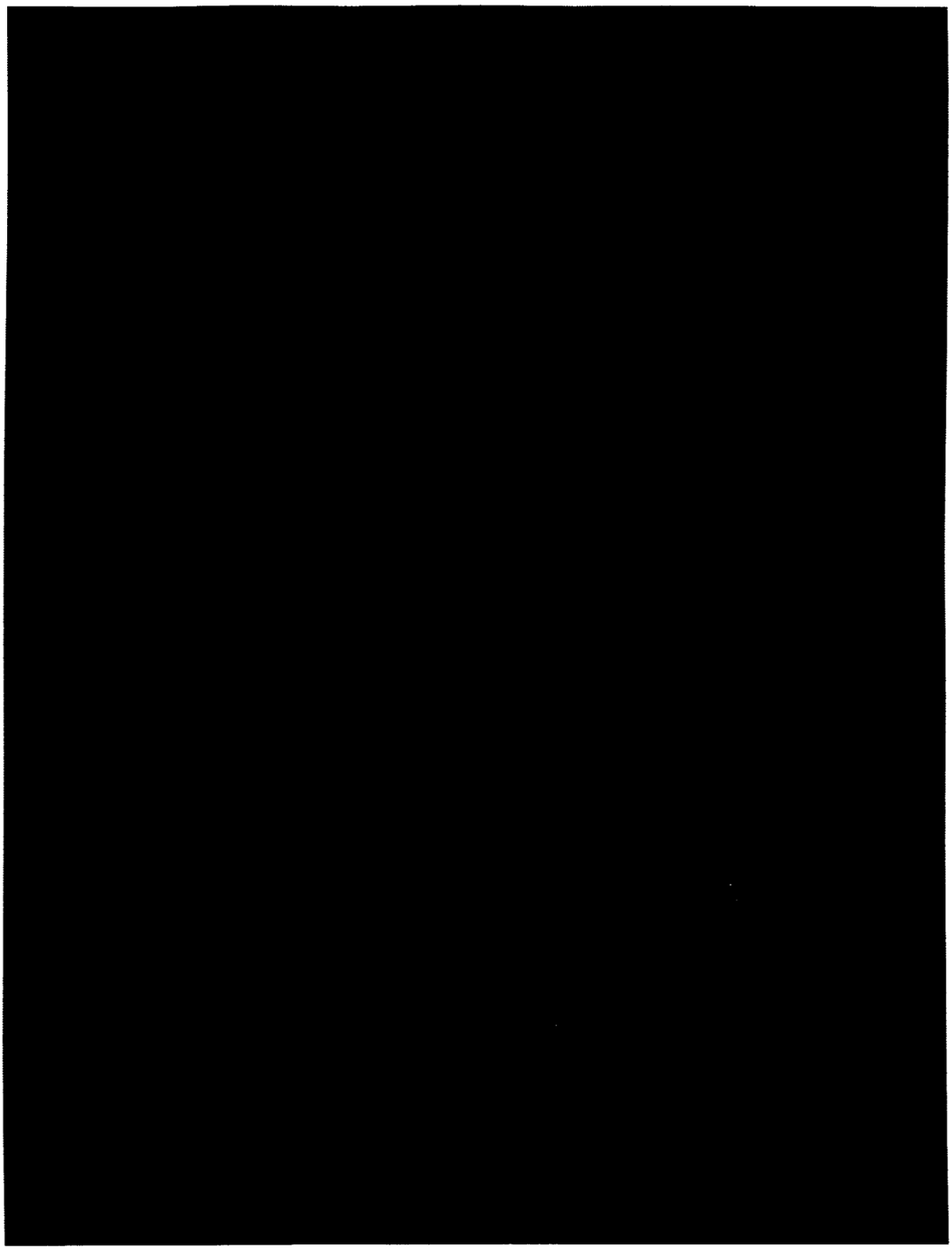

Fig. 1 - SEM of Eight Site Probe used for Stimulation in Guinea Pig.

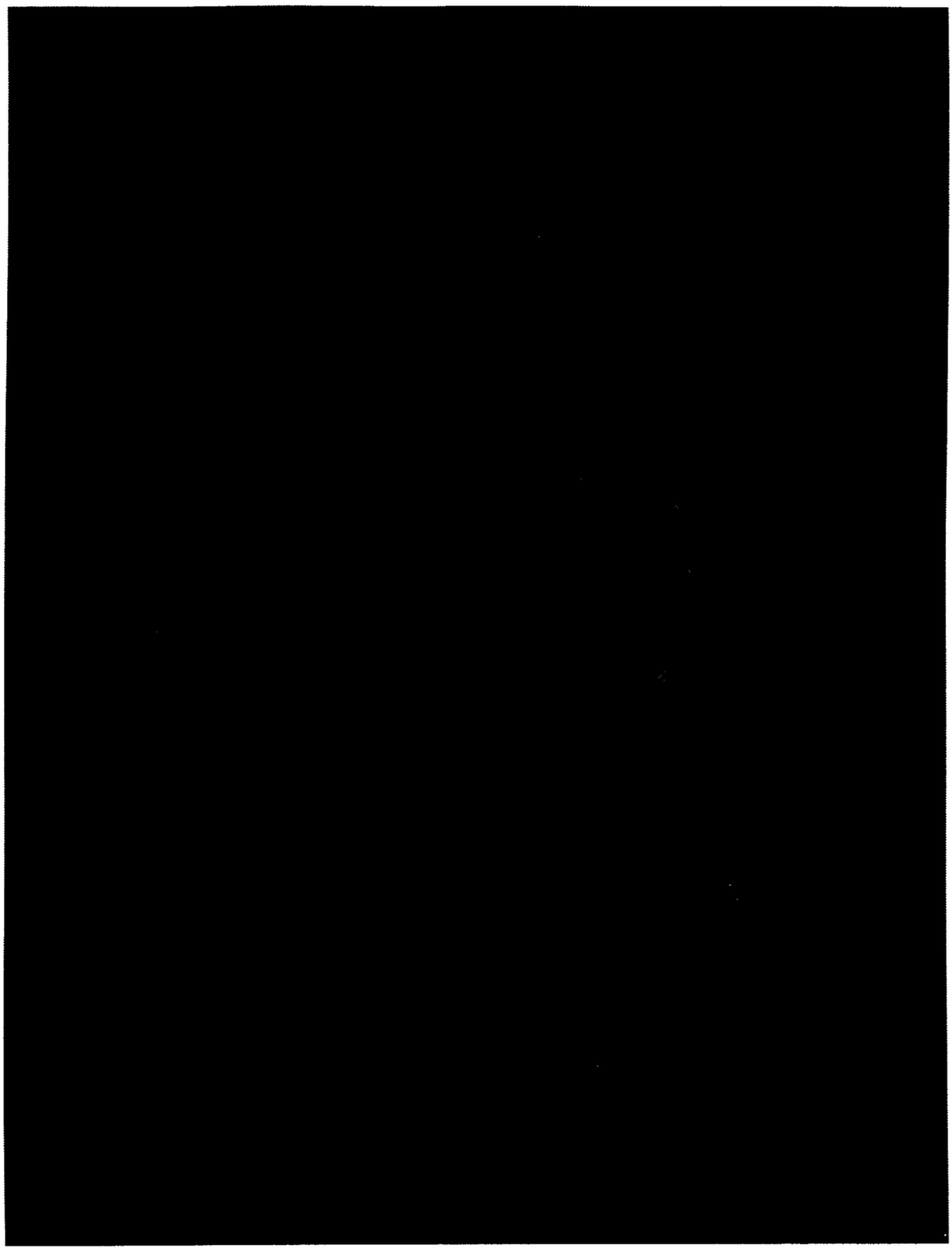

Fig. 2 - SEM of chronically implanted 400 μm^2 site.

Long-Term Studies

One guinea pig from the summer '95 experimental series was allowed to survive in order to test the longevity of the chronic stimulating electrode. The test was completed as described above (i.e., one week of stimulation), but electrode integrity was tested at weekly intervals after the completion of the stimulation. To date, the electrical characteristics of the electrode, while not exactly stable, indicate that five of eight sites are still viable. The site sizes are as follows: site 3 - 400μm^2, site 4 - 800μm^2, sites 5,8 - 1200μm^2 , and site 6 - 1600μm^2. Impedance and access resistance measurements for all the sites are shown below (Figs. 4 and 5). A CV curve for one site has also been included in Fig. 3.

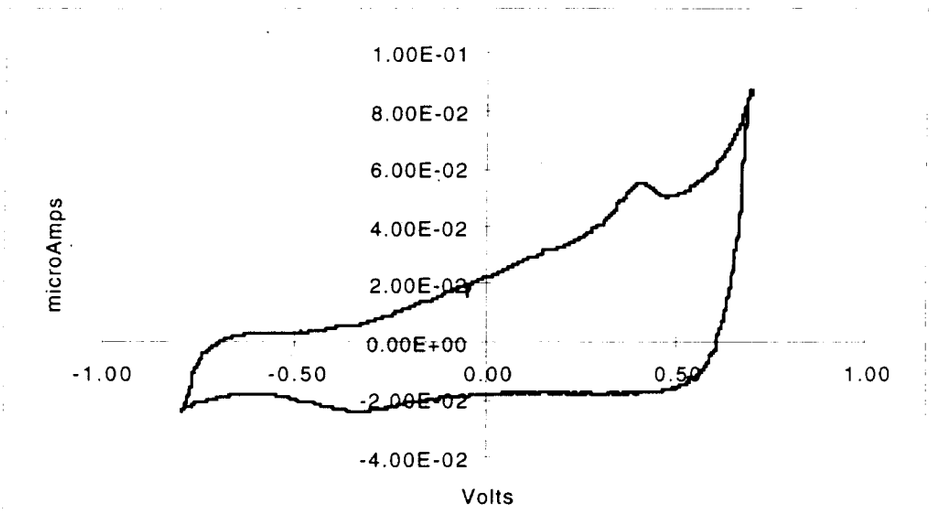

Fig. 3: *In Vivo* CV of 1600μm^2 site, 18 weeks post implant.

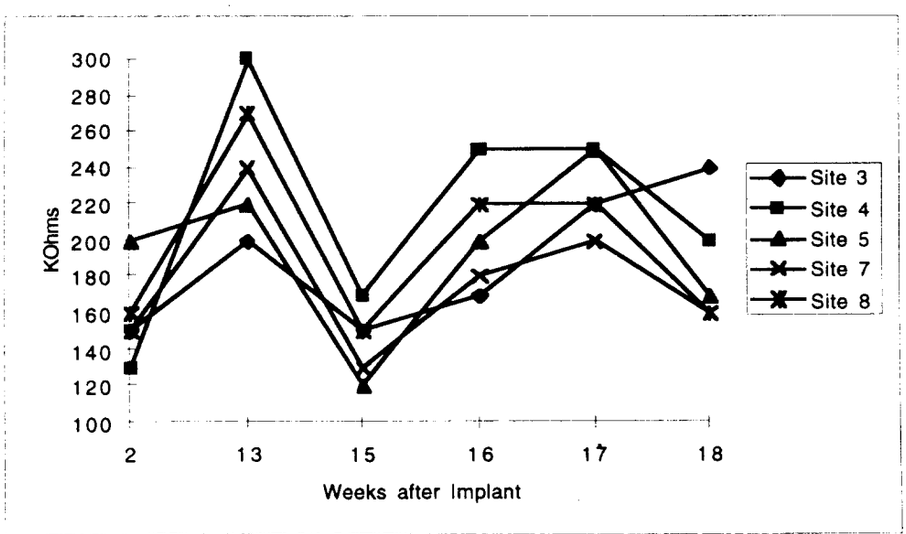

Fig. 4: *In Vivo* 1kHz impedance of a multisite electrode.

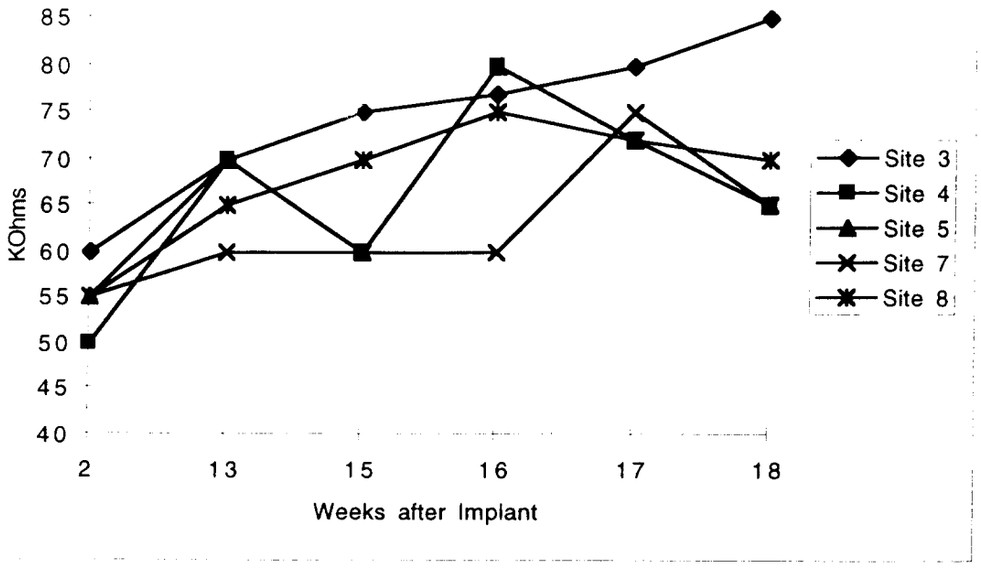

Fig. 5: *In-vivo* access resistances of a multisite electrode.

These data point out some deficiencies in our data collection and analysis capabilities. The following discussion details these problems and how they will be addressed. Our impedance measurements were all taken at 1kHz with a 5μA sine wave. In order to get a more complete picture of the impedance of the different components of the system, a spectrum of frequencies should be used, but the range of frequencies available is limited by our instrumentation. The D/A board we currently use can produce a fairly smooth sine wave up to only 5kHz, which limits our ability to analyze the high frequency characteristics of the system. Also, a constant voltage should be used to test electrode impedance to limit inaccuracies from electrochemical reactions. When applying current, the voltage developed is dependent on the impedance of the electrode. The voltage is also dependent on the duration of the current, so low frequency signals develop a larger voltage than higher frequencies. Large voltages may induce electrochemical reactions which will also affect the impedance measurements. One could adjust the current level used at different frequencies to keep the voltage at a constant level, but this is a cumbersome solution. Furthermore, our present instrumentation does not allow us to control the potential of the electrode (potentiostatic measurement). This has been shown to dramatically affect the impedance of the iridium oxide. Impedances measured without complete control of the potential have been shown to drift and should not be considered reliable.

Access resistance is also difficult to measure with our present instrumentation. Access resistance can be measured readily *in vitro* by dividing the initial voltage drop by the initial current flow. The voltage across an electrode in saline exhibits a distinct break point between voltage drop from electrolyte resistance and double layer charging, facilitating this measurement (Fig. 6). However, when the same measurement is taken *in vivo*, the break point between initial voltage drop and capacitive build-up is ambiguous (Fig. 7). These data were taken from the same electrode site, immediately before and after implantation (monopolar stimulation, 1600μm^2 site). These experiments produce data that

suggest that the access resistance of a 400μm² site is not much greater than that of a 1600μm² site, a result that conflicts with intuition and with *in vitro* results. While the measurements we made *in vivo* were consistent with respect to the method in which they were acquired and could be used to qualitatively track a particular experiment, these numbers are probably not good quantitative values for access resistance.

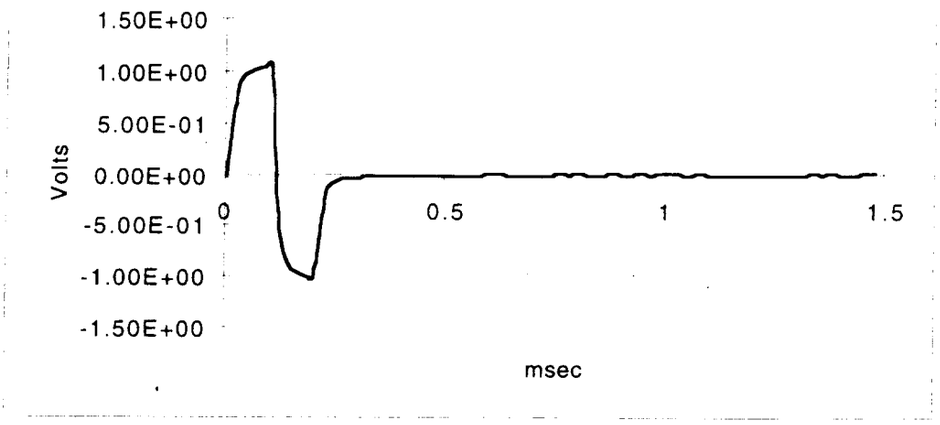

Fig. 6: Voltage drop in vitro to a 50μA pulse.

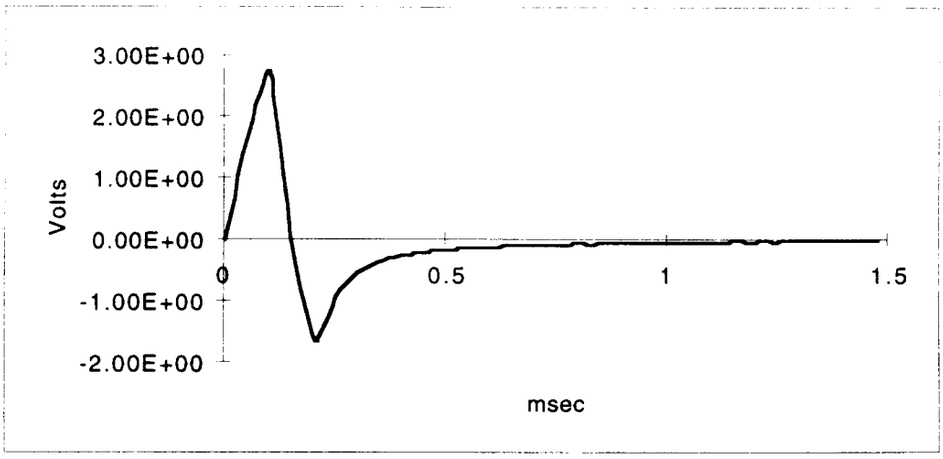

Fig. 7: Voltage drop in vivo to a 25μA pulse.

Plans for Improving the Electrical Measurements

In order to improve our data collection capabilities, we will use an impedance spectroscopy system designed to make electrochemical measurements. The system, which should be operational this quarter, features a potentiostat and a frequency response analyzer. The potentiostat will provide the interface to the electrode. It uses a standard three-electrode setup to control electrode potential and measure electrode current. The excitation waveform will be supplied by the frequency response analyzer (FRA). Similar to a phase-lock amplifier, the FRA will compare a reference signal, which is also input to the electrode, with the output signal from the electrode to get magnitude and phase

information about the electrode-tissue system. The potentiostat will allow us to measure impedance in a consistent fashion by controlling the operating point of the electrode. At high frequencies, the electrode impedance is negligible, and any potential drop will be due to series resistance. Therefore, access resistance can also be measured as the impedance at high frequencies (the resistance of the conductor path to the electrode site is assumed to be known). The FRA can process signals up to 2MHz, higher than we will probably require. Additionally, both instruments are controllable via GPIB, so this impedance system can be used in automated testing during a chronic stimulation experiment.

Additional improvements were made to software used for data collection. A program has been written in LabVIEW to collect evoked responses. This program allows a user to construct strength duration curves and input output functions by examining evoked responses. Figure 8 shows an example of the auditory evoked responses recorded from head screws. The stimulus was an acoustic click. The auditory brainstem response and the middle latency response were recorded and are indicated on the graph. A P15 Grass amp was used to amplify and filter the signal (gain 1000, bandwidth 3Hz - 3kHz). Additional amplification is available on the A/D board and can be controlled through software. The signal shown was averaged over 500 presentations. Evoked response recording has been incorporated into the chronic stimulation program as well, with the intent of recording responses to electrical stimulation in the cochlear nucleus of guinea.pig during the course of a chronic stimulation experiment.

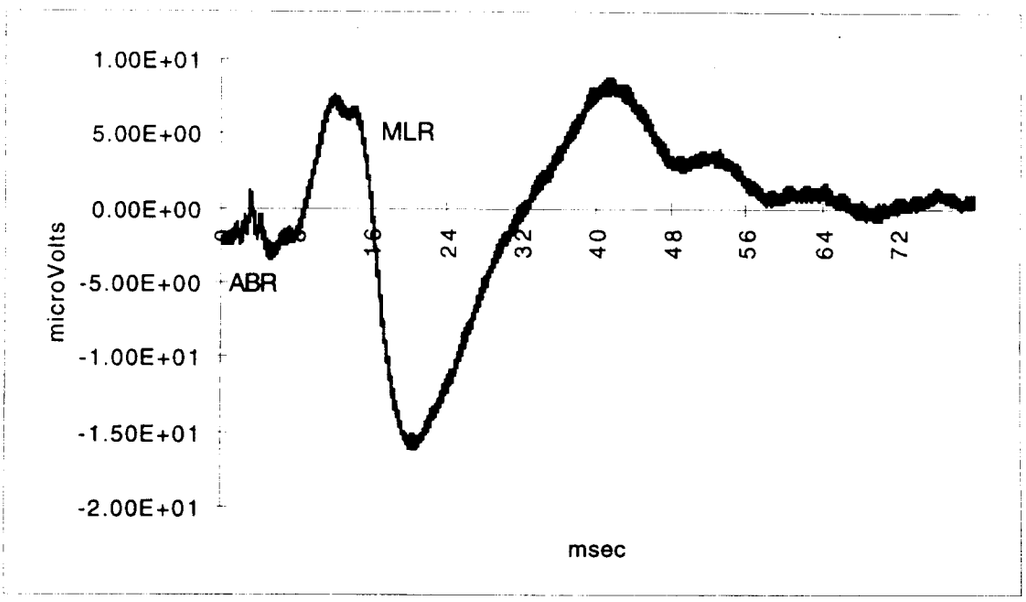

Fig. 8: ABR and MLR potentials in response to acoustic stimuli.

During the coming quarter, we hope to resume chronic implants. New instrumentation should allow quantitative data to be collected from these experiments. Also, evoked responses from electrical stimulation should be available in the next quarter. The long-term implant mentioned above will be monitored. Finally, tissue samples from last summer's experiment will be examined.

3. *Contact and Interconnect Development*

We are currently putting a concentrated effort into the development of several contact and interconnect technologies which have not previously been in common use in our fabrication facility. The development of these alternative processes has been motivated by contact resistance problems and the need for a lower-resistance interconnect on many of our probes.

For the past several years, we have been plagued with inconsistent results from our circuit contacts. Unacceptably high contact resistances have reduced yield on our active probes as well as in other circuit processes. This has led to a plan to move away from direct Al-Si contacts, which are now standard in our processes, to the use of other materials as plugs. The properties of the contact types that we are considering have been reported before and are now commonly used in industry. Based on previously reported results, we have elected to first investigate the use of TiN and Ti:W plugs. TiN is an excellent passive diffusion barrier and is known to demonstrate low electrical resistivity and high chemical and thermal stability. Ti:W, sputtered in a N_2 ambient in order to "stuff" the material's grain boundaries, also acts as a good passive barrier. In addition, Ti:W is reported to demonstrate good adhesion to SiO_2 and good step coverage, as well as a low contact resistance after annealing. We have ordered sputtering targets for high-purity TiN and Ti:W and will begin experiments with these materials during the coming quarter. These materials can make stable ohmic contacts to both p- and n-type silicon and are consistent with the use of both metals and silicides as interconnect materials. Fig. 9 shows a cross-section of a contact in which a passive diffusion barrier is used between the interconnect and the silicon substrate.

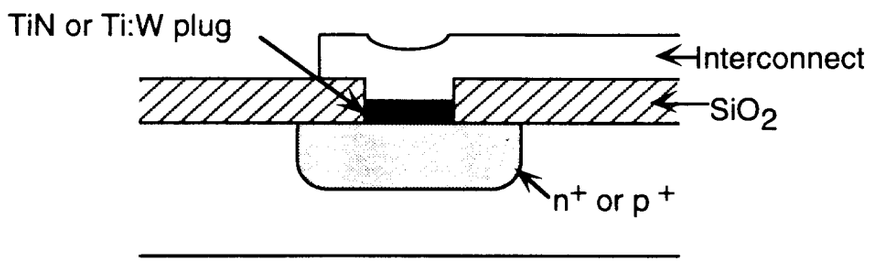

Fig. 9: Cross-section of a contact in which a passive diffusion barrier is used between the interconnect material and the silicon substrate.

There are many applications which will benefit from the development of a low-resistance interconnect technology in our laboratory. Examples of these applications include probe power lines, which must carry relatively high levels of current or provide very low-resistance (noise-free) ground references, and long interconnect lines such as those used on our ribbon cable probes. The requirements for the interconnect are that it 1) has a resistance of less than 1Ω/square, 2) demonstrates good adhesion to the upper and lower dielectrics, 3) can withstand the mechanical stresses induced during subsequent processing or during the implantation of ribbon cable probes, and 4) makes ohmic contact to n- and p-Si for use as a circuit interconnect. The materials which we have chosen to begin experimenting with are the refractory metal silicides, $TiSi_2$ and $TaSi_2$. Both materials have very low resistivities and a high propensity to oxidize, which improves their adhesion to the dielectric and helps reduce leakage. We will begin experimenting with different

process flows to investigate the properties of salicides, polycides, and metal-silicide "sandwiches" formed with Ti and Ta during the coming term. Figure 10 shows some of these structures.

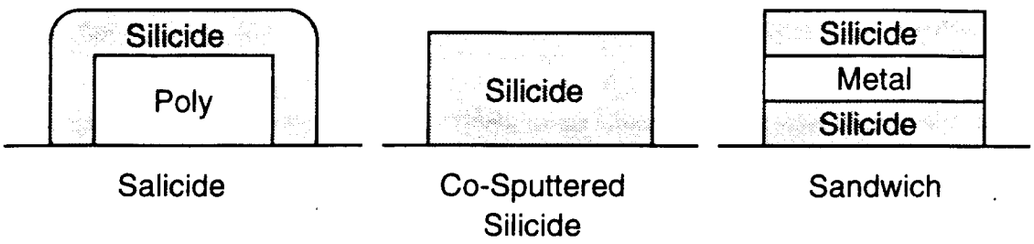

Fig. 10: Three different methods for fabricating low-resistance interconnect using refractory metal silicides.

Layout of a test die for these experiments is currently underway, and during the coming quarter we will concentrate on the characterization of the previously discussed contact and interconnect materials. It is our aim to have chosen the most appropriate materials and process steps for our contacts and interconnects by the end of the next quarter, so that we can then begin integrating them into all of our process flows.

4. Active Stimulating Probe Development

During the past quarter, work on the active stimulating probes focused mainly on the debugging, simulation, and redesign of some portions of the STIM-2 circuitry (in particular, the current DAC), and the initial design of a new probe, STIM-2b. Comments on work with each of the active probes are given below.

STIM-1B

STIM-1b is the simplest version of the active stimulating probes. The probe simply uses a four bit counter to select one of sixteen sites. The selected site is connected to the analog data input pad through a pass-gate transistor. The counter is incremented by a positive pulse on the clock-in line. The counter can be reset to the first site by strobing the clock line negative. This is a monopolar probe which simply acts to steer an externally-generated current to a selected site. The functionality of this device is dependent mainly on the correct operation of digital site-selection logic. The lack of analog circuitry makes the design very robust with regard to its dependence on process parameters.

The STIM-1b probes have been found to function exceptionally well *in-vitro*. They have demonstrated the capability of operating at clock speeds as high as 10MHz. The STIM-1b probes have also been used in simple in-vivo experiments. The results of the in-vivo testing have clearly demonstrated the potential of these probes as a simple multisite tool. During the previous quarter, little additional work has been done with the STIM-1b probes due to their short supply. We will begin a new CMOS fabrication run in order to produce more of these probes during the coming quarter.

STIM-1A

STIM-1a is a first-generation probe with the capability for on-chip bipolar current generation. The user can source and sink current by selecting any two of its sixteen 450μm^2 sites, one as the current source and the other as the current sink, by clocking in a 15b data word and latching it with a negative clock strobe. The first four bits specify the site address of the current sink electrode, the next four bits specify the site address of the current source electrode, and the last seven bits specify the amplitude of the current to be driven, which can be as high as 254μA with a 2μA resolution.

Etched out STIM-1a probes have been previously tested *in-vitro* and function close to specifications. STIM-1a has been demonstrated to operate at clock speeds as high as 3.3MHz while driving current in a saline bath; this upper frequency limit appears to be related to the inability of the external electronics to pull the clock line low enough at high speed when immediately surrounded by positive pulses. As with STIM-1b, during the previous quarter, little additional work has been done with the STIM-1a probes due to their short supply. These probes will also be produced in the next CMOS fabrication run.

STIM-2

STIM-2 is a second-generation probe that it significantly extends the capabilities of the first-generation probes in many areas. STIM-2 incorporates: 1) flexible interconnects, which allow the rear, circuit-containing, portion of the probe to be folded flat against the cortical surface to reduce the probe height above the cortical surface in an implant, 2) new circuitry for power and area reduction while increasing functionality, 3) a front end-selector which allows 8 of 64 sites to be driven simultaneously, thereby implementing electronic site positioning; and 4) compatibility with use in a multi-probe three-dimensional array.

We are working with STIM-2 probes from the past fabrication run so that we can identify any other problems that may exist with this probe and correct them before the next fabrication run. The output n-channel DAC bias string was the first circuit block identified for modification. Yield of this probe has been substantially reduced due to chemical attack of two of the bonding pads, especially the ground pad, during the final EDP etch. The problem on these two particular pads is that contact is being made between the polysilicon leads and the Ti/Ir pad using an intermediate aluminum layer as shown in Fig. 11. The aluminum forms hillocks during the LTO deposition step due to the high stress in the Al at the elevated temperature. The Ti/Ir layer is then deposited on the aluminum in the site/pad definition step. Unfortunately, the Ti/Ir layer cracks over the sharp hillocks, allowing the final EDP etch to attack the underlying aluminum and polysilicon, thereby destroying the pad. We have previously attempted to overcome this problem using rapid thermal annealing (RTA). As a 'quick-fix', we are now looking at covering the Ti/Ir with a thick layer of Cr/Au in order to seal any cracks in the Ti/Ir, thus effectively protecting the underlying Al from the final EDP etch as in Fig. 12. In any future redesigns of the probe, we will change the pads so that contact between Ti/Ir does not occur directly over aluminum, which should totally eliminate the problem.

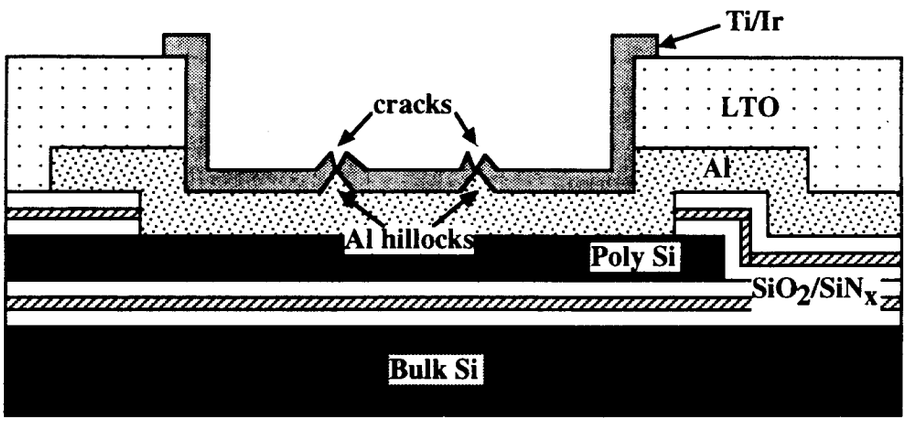

Fig. 11: A cross-section of the STIM-2 bonding pads which have a high failure rate due to hillocking in the Al layer, which causes cracking in the Ti/Ir overlay.

The main focus of work during the past quarter has been on improving and redesigning the output DAC of STIM-2. The operation of the present design has been re-simulated and re-evaluated with the emphasis on maintaining charge balance of the stimulation current. In order to realize optimal charge balance, it is necessary that the sourcing and sinking currents are as perfectly matched as possible. A look at the circuit, shown in Fig. 13, shows that the sourcing and sinking sections of the DAC are biased by two different reference currents. This design has the advantage of very low power dissipation by only having one reference current 'on' across the 5V supply at any time during stimulation. The control circuit also uses the reference currents as a means of selecting the sourcing or sinking section of the DAC. The problem is that having two different reference currents means the output currents will not necessarily be matched if the supply voltages are not matched or if the circuit parameters of a given fabrication run do not match those used in designing the DAC. It is possible to match the sourcing and sinking currents by individually adjusting the supply voltages, but this would require manually adjusting the supply voltages for each probe. It is better to implement a design in which the circuit delivers sourcing and sinking currents that are inherently matched in spite of any

process parameter variations and without having to adjust the supply voltages. It might be noted, however, that this matching is most critical on probes such as STIM-1a, which generate "matched" bipolar outputs. All of these probes will normally require calibration if precision current levels are required, and storing two correction tables (for sourcing and sinking) instead of just one is not a major addition. Nonetheless, since the DAC circuitry is being redesigned to improve its sinking capability anyway, its matching performance is being improved as well.

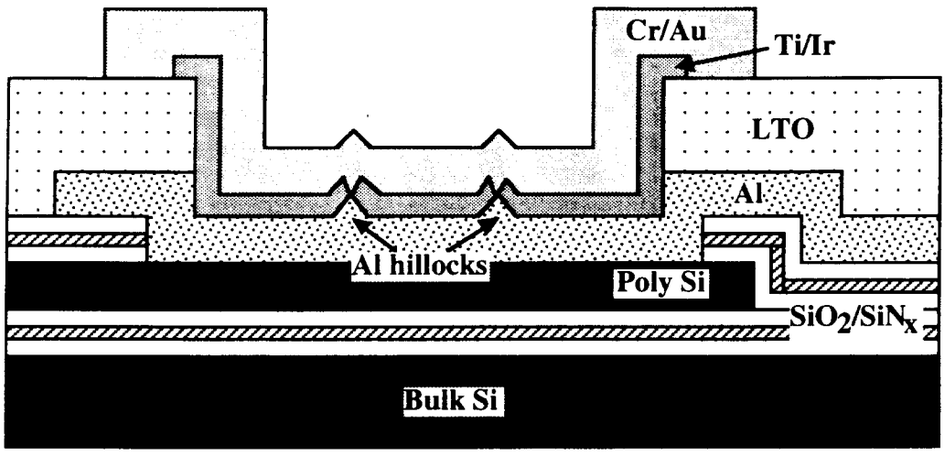

Fig. 12: Cross-section of a failed STIM-2 bonding pad inlaid with a possible 'quick-fix' layer of Cr/Au to seal the Ti/Ir cracks and thus protect the underlying Al from the final EDP etch.

Current matching can be easily accomplished by biasing both sourcing and sinking sections of the DAC to the same reference current as in Fig. 14, using a circuit much like that used on the STIM-1a probes. In order for a DAC circuit to be usable in STIM-2, it must have ability to operate sourcing and sinking sections independently under the direction of the control circuitry. The simple circuit of Fig. 14 does not have the capability of independent operation. There is more than one way of realizing independent control, but the design presently being evaluated via simulation, shown in Fig. 15, is a modified version of the simple current mirror of Fig. 14. The common reference current is mirrored into two independent secondary reference currents, $I_{n\text{-}ref}$ and $I_{p\text{-}ref}$, which can be turned off or on by the control circuitry, thereby biasing the output current transistors. This design has the disadvantage of greater complexity, larger layout area, greater power dissipation (an additional reference current). More importantly, because of the non-ideal current mirroring in real circuits, there is the possibility of greater mismatch of the output currents due to mirroring the current twice.

Another possible implementation is shown in Fig. 16. This design is nearly the same as the original STIM-2 design except that it only uses a single reference current and turns off sourcing/sinking by bypassing the appropriate mirroring transistor with a matched transistor string. The advantage of this design is that the reference current can be completely turned off if the DAC is not in use. The disadvantages are the added circuit complexity and layout area and possible variations in the reference current due to transistor mismatch in the bypass strings. Seven bit resolution will likely be impossible in this DAC configuration because of this mismatch.

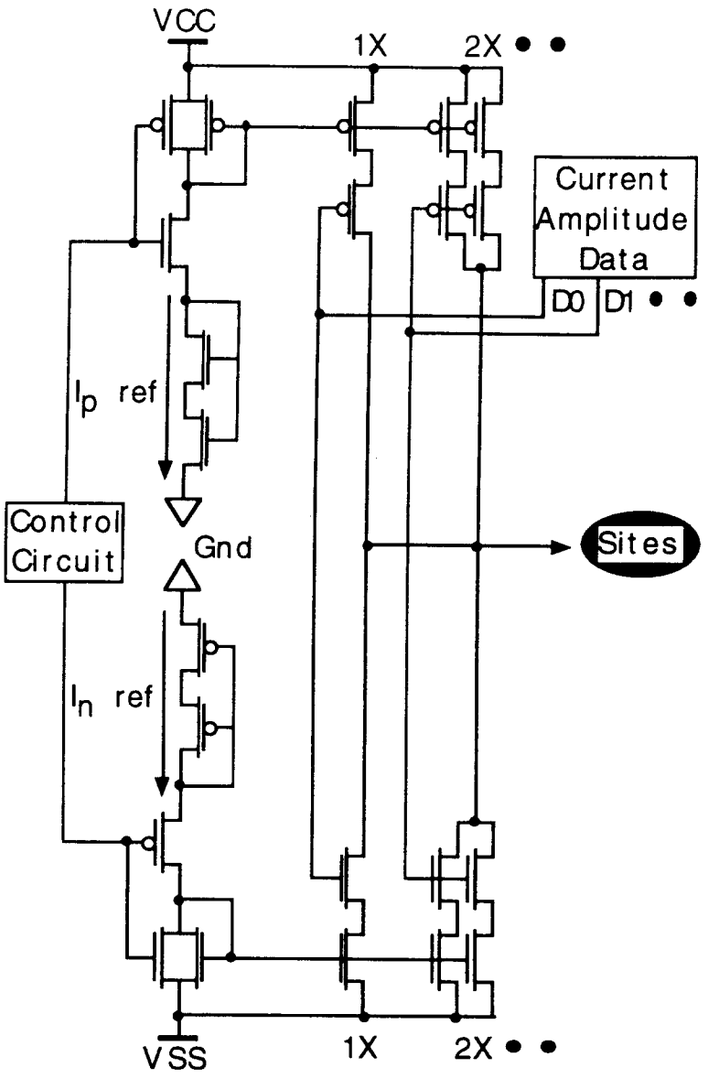

Fig. 13: Schematic of the present STIM-2 output DAC design.

Another possible implementation being considered is shown in Fig. 17. In this configuration, the reference current is on 'full-time' unless additional control logic is included to operate a switch in the reference current string. The advantage is that the secondary reference currents are eliminated thereby reducing the power dissipation. Removing the secondary references also reduces the layout area, but the effect of having a transistor switch in the mirror path may degrade the matching of the output currents. It may be necessary to use a full pass-gate as the switch if the bias point is comparable to the threshold voltage of the individual transistors. It is expected that the bias point will be far enough away from the supply voltage so that a full pass-gate will not be necessary, but that decision will be made after full simulations are complete. On the whole, this is a very attractive scheme for implementing the biasing for the STIM-2 DAC.

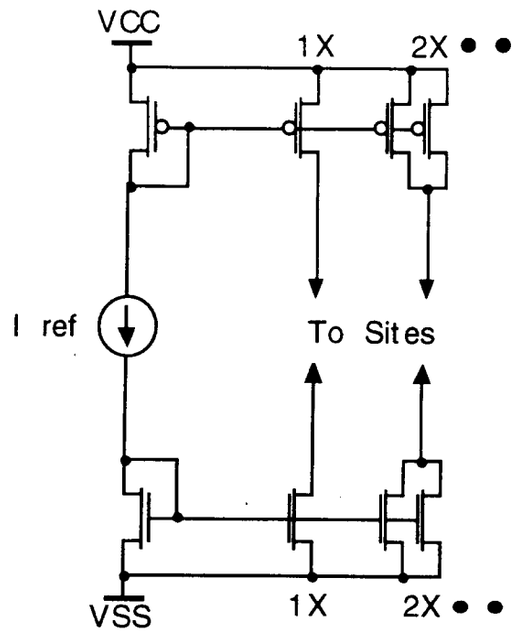

Fig. 14: A simple current mirror design which gives good matching between sourcing and sinking currents by mirroring the same reference current.

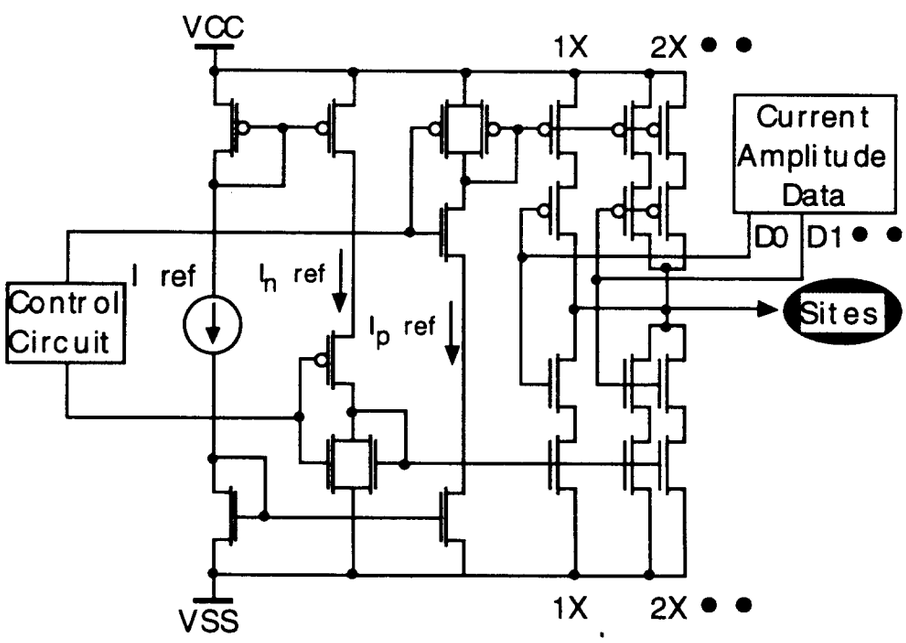

Fig. 15: Schematic of the circuit presently being evaluated as a future implementation of the STIM-2 DAC. The design utilizes secondary reference currents for the sourcing and sinking portions of the which can be independently switched on and off.

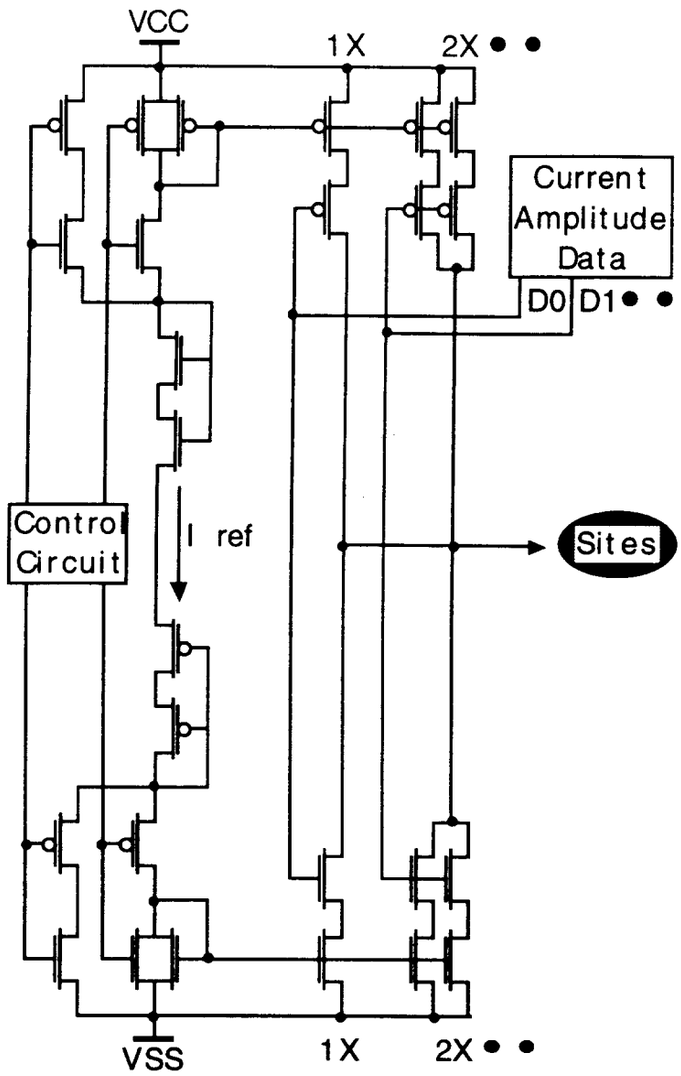

Fig. 16: Schematic of an implementation of the STIM-2 DAC utilizing bypass strings for on/off control of the sourcing/sinking functions.

STIM-2B

STIM-2b is a second-generation four-channel 64-site version of the simplest active stimulating probe, STIM-1b. The probe uses a 20b shift register to load four four-bit addresses which are decoded to select one of sixteen sites per channel as shown in Fig. 18. The selected site is connected to the analog data input/output pad through a pass-gate transistor to allow 'externally-generated currents to be 'steered' to the selected site. A flag bit is included with the channel address in order to select between stimulation and a newly added recording function. The flag bit selects either a direct path between the I/O pad and the site or elects the path through a buffer amplifier for recording. A power-on-reset circuit (POR) sets all of the circuits to a predefined startup state and connects all of the sites to the I/O pads in order to facilitate activation of all of the sites in parallel. The first clock pulse

knocks down the POR signal, and the probe subsequently begins functioning normally. The POR state can also be initiated by strobing the clock line low using CSTB. A strobe on the address line, ASTB, resets all of the addresses to site zero and clears the flags (stimulation mode). Additional circuitry is included with site zero so that if the address line is held low, ASTB is maintained and all sites are disconnected, thereby allowing the probe leakage current to be measured. The functionality of this device is dependent mainly on the correct operation of the digital logic circuitry for selecting the correct site for current delivery or recording. The recording buffer amplifiers are essentially the only analog circuits present, and their unity gain design should make them very predictable and immune to variations in process parameters. The minimal amount of analog circuitry makes the design very robust with regard to its dependence on process parameters.

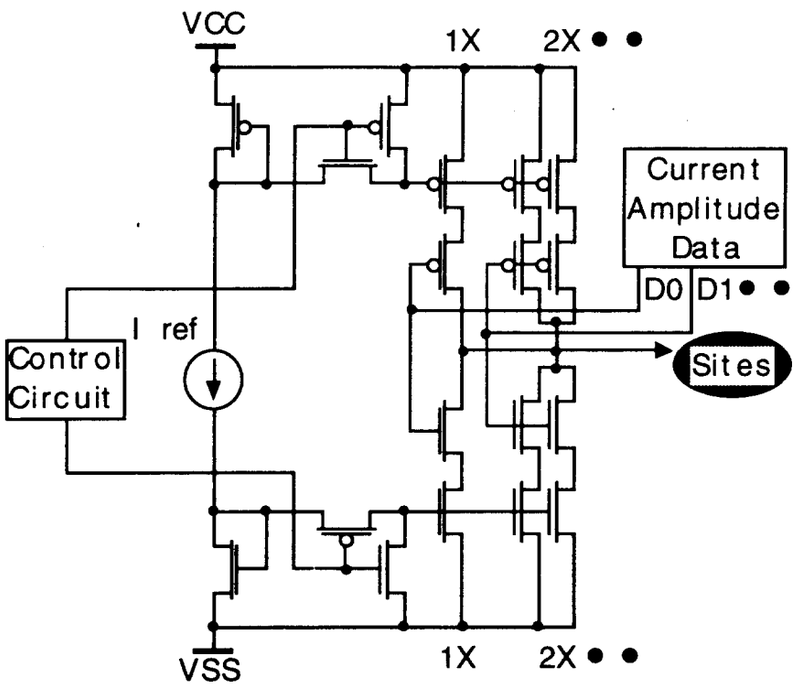

Fig. 17: Schematic of an implementation of the STIM-2 DAC which uses a switch in the mirror path to realize on/off control of the sourcing/sinking sections of the DAC.

During the coming quarter, we plan to complete the evaluation of the various DAC designs for STIM-2 and finalize a few other changes that have been proposed previously, including the use of a bonding pad dedicated to recording and correction of the faulty bonding pad structure. We also plan to implement the 'quick-fix' on the present faulty STIM-2 bonding pads in order to utilitize the wafers still remaining from the last run. A new CMOS run will also be started so that the supply of STIM-1a and STIM-1b probes can be replenished. We also plan to start the simulation and layout the new STIM-2b probe.

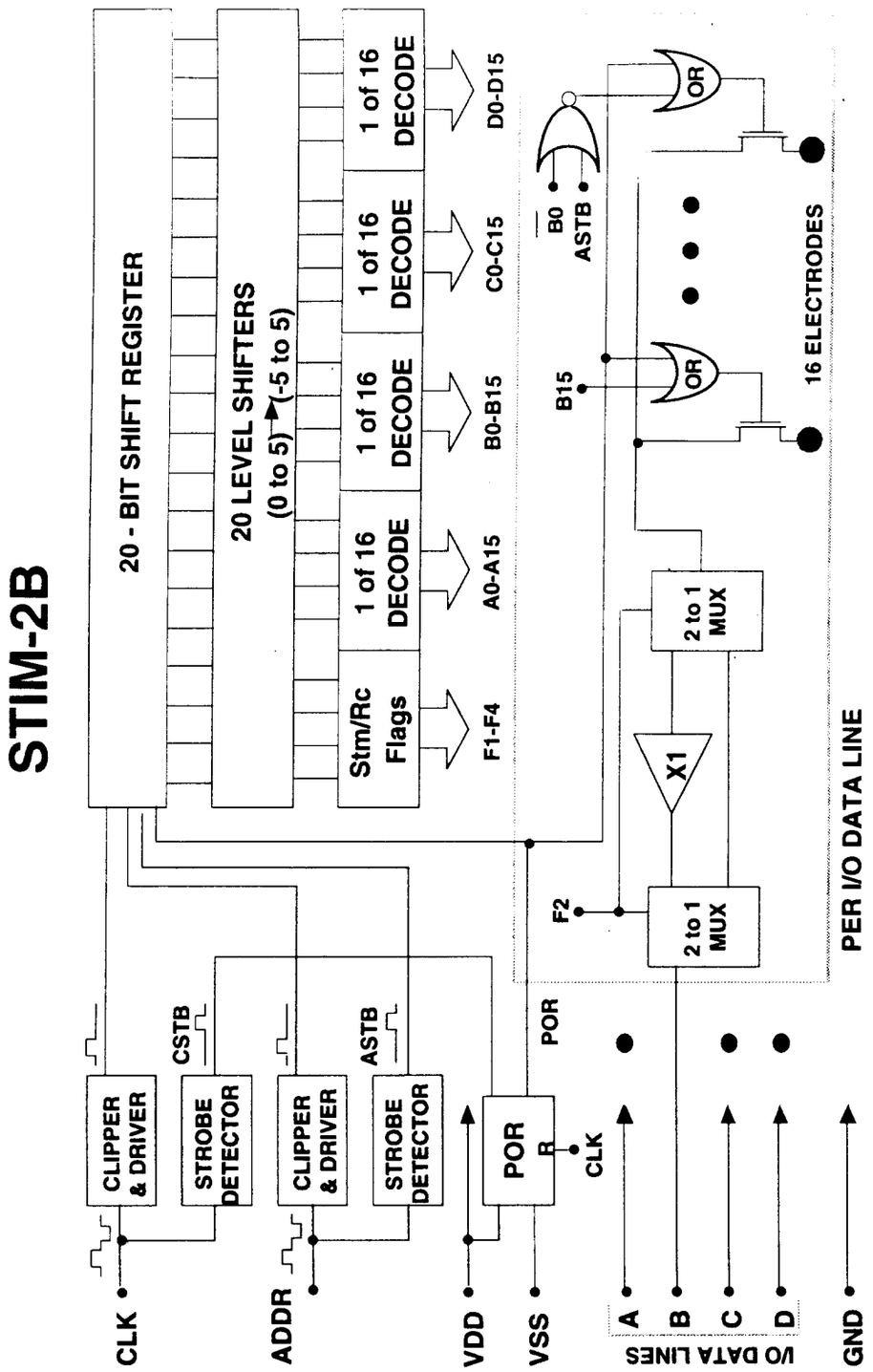

Fig. 18: Block diagram of the STIM-2B probe.

5. *External Electronics for Stimulating Probes*

With external hardware systems soon to become available, the focus of our work during the last quarter was on the development of a robust and user-friendly graphical interface to this hardware. To support the short-term needs of stimulating probe users, a specialized interface that only supports the generation of pulsatile waveforms was developed. This program allows control over both duration and amplitude of the two phases of a bipolar pulse. Bipolar pulses can be sent as single events, or as a repetitive pulse train with programmable repetition frequency. The stimulation site can be configured, as can the type of probe being used (STIM-2, STIM-1, or STIM-1a), and the data interface bit rate (4.0MHz or 0.4MHz). As an aid in generating frequently-used waveforms, sets of pulse parameters can be given a name and the entire named set can be saved in a list from which the user can later select a previously-stored pulse set. This list can additionally be saved to disk, so that it may be loaded in a future session.

This user-interface program is now complete. It remains, however, to write support software that runs on the Chimera board (the PC plug-in board that acts as the interface between the PC and the stimulating probe). This software will accept commands from the user-interface program and actually generate the appropriate waveforms. It is expected that this software component will be completed early in the coming quarter.

In the hardware development arena, we are building five complete external interface systems for use with the external stimulating probes. These systems are due to be completed in the near future. We expected to have these systems ready by the end of this past quarter but their construction was slowed by an unexpected delay in acquiring the necessary electronic parts. All parts have now arrived, however, and we expect to receive the assembled systems shortly.

Finally, we are considering future directions for the next generation of external interface systems. One concern that has been raised is that the current hardware is wedded to a particular family of stimulating probes and is unable to communicate with possible new probe designs. When the current external hardware was first designed, upward compatibility was not a major design issue. Now, however, we realize that maximum compatibility with a wide variety of probe interfaces is desirable. To this end, we are considering replacing one of the dedicated hardware components (the Chimera daughterboard) with software that can be programmed to communicate with probes in any fashion. This will most likely require the use of a different PC plug-in card (to replace the Chimera) with more processing power and a greater number of interface channels.

6. *Conclusions*

During the past quarter, work on the development of thin-film micromachined stimulating electrode arrays has gone forward in a number of areas. Three additional process runs of active and passive probes have been fabricated for internal and external users. Histological studies of an 8-site passive probe implanted for approximately six weeks showed biological material adhering selectively to each of the exposed sites, all of which passed some current during the implant period. Another electrode recovered from a similar test, was not used for stimulation for at least four weeks prior to sacrifice and did not show tissue accumulation on any of its sites. For another chronically-implanted multisite probe, the in-vivo cyclic voltammetry curve, the in-vivo impedance, and the in-vivo access resistances remained relatively stable and viable after 18 weeks of implantation. The instrumentation for making many of these measurements is being upgraded to allow

impedance spectroscopy on the electrodes along with improved data collection capabilities. Work has also begun to improve the contact and interconnect structures used on the probes. This includes the use of TiN and Ti:W contact plugs and refractory metal/silicide low-resistance interconnects. Sputtering targets for the selected materials have been ordered and a test mask set to allow technology development is in design.

The current-generation circuitry used on STIM-2 is being redesigned to allow more reliable current sinking capabilities and to ensure more accurate matching between the source and sink currents. A number of different circuit designs are being simulated, and a final design should be completed during the coming term. Yield problems associated with an aluminum hillocking problem on some of the bonding pads in STIM-2 are also being corrected. The design of a new 64-site 4-channel active stimulating probe is also nearing completion. This device uses a 20b input word to control four 16:1 site selectors, resulting in a 64:4 site multiplexer. The selected site from each of the four groups can be either passed directly to an output pad for connection to an external current generator or can be passed to the pad through an on-chip preamplifier, allowing neural activity in the vicinity of the site to be monitored externally. A new fabrication run of the previous STIM-1a and STIM-1b probes has begun and a run of revised STIM-2 probes and STIM-2b will begin during the coming quarter.